RSC Advances

ROYAL SOCIETY OF CHEMISTRY

www.rsc.org/advances

A Facile Modification of Poly sulphone based Anti biofouling Anion Exchange Membrane for Microbial Fuel Cell Application

*Elangovan Mahendiravarman and Dharmalingam Sangeetha**
Department of Mechanical Engineering, Anna University, Chennai-600 025, India
*Corresponding author Email: sangeetha@annauniv.edu
Tel No: +91-44-22357763, Fax No: +91-44-22357744

Abstract

The present study aims at developing an anti biofouling anion exchange membrane based on quaternized poly sulphone (QPSU) having functionalized graphene oxide (FGO) in proportions. Solvent-casting method is used to fabricate the nanocomposites QPSU, QPSU/GO and QPSU/FGO. The changes in material properties due to FGO inclusion are studied in detail. The membranes are characterized by FTIR, Raman spectroscopy, SEM, XPS, XRD and impedance spectroscopy. Anti adhesion and antibacterial tests are also done. The agar plate test corroborates that QPSU/FGO has better anti-bacterial property than QPSU and QPSU/GO. Out of the five, QPSU/FGO-1.0 % only was able to register a maximum power density of 1036 ± 15 mW m^{-2} and current density of 2880 ± 70 mA m^{-2}. The same for other samples were relatively lower, ie it was 945 ± 8 mW m^{-2} and 2780 ± 48 mA m^{-2} for QPSU/FGO-0.5%, 874 ± 4 mW m^{-2} and 2300 ± 27 mA m^{-2} for QPSU/FGO-2.0% , 805 ± 2 mW m^{-2}, 2120 ± 13 mA m^{-2} for QPSU and 576 mW m^{-2}, 1800 mA m^{-2} for AMI 7001. A comparison between the prepared ones and commercially available AEMs like AMI-7001 reveals that the membrane QPSU/FGO-1.0 wt.% has the least resistance with enhanced efficiency, making it an efficient anti bio fouling anion exchange membrane for its use in long term applications.

Keywords: Anion exchange membrane, Functionalized graphene oxide, Quaternized polysulphone, Nanocomposite membrane, Anti biofouling

1 Introduction

Microbial fuel cell (MFC) is a type of electrochemical cell which convert biodegradable organic waste into electricity directly using bacteria.[1,2] Basically an MFC consists of an anaerobic anode chamber and an aerobic cathode chamber separated by an ion exchange membrane which allows only selective ions to pass through. The wire connecting anode and the cathode externally completes the circuit. At the anode the oxidation of substrates by microorganisms produces electrons and protons and transport the generated electrons to the cathode by diverse respiration processes. Due to the potential difference between cathode and anode, electrons are transferred to the cathode through the external circuit.[3, 4]

A number of studies had been undertaken in the past to enhance MFC performance by varying technical and engineering aspects.[5] Though several milestones have been crossed in power generation, the practical applications are only a few due to unstable system performance, low electron recovery, and high cost of commercially available ion exchange membranes and cathode catalyst.[6] Moreover membranes like Nafion has several limitations such as high cost, poor proton transfer, and increased internal resistance due to easy fouling (hydrophobic nature) etc.[7] The poor proton diffusion from anode to cathode chamber lowers the pH, which affects microbial action and ultimately ends up in poor system performance.[8] MFC operation without a membrane may provide high power densities but at the loss of coulombic efficiency due to uncontrolled oxygen diffusion and substrate crossover. [9] As alternates to high cost ion exchange membranes, several separators such as J-cloth, glass fibre, nylon mesh and ceramic membranes were developed[5, 10, 11, 12] but none found suitable for multiple reasons such as biodegradation, low columbic efficiency (CE), high internal resistance and high cost.[5, 12 ,13]

Kim *et al*. examined the performance of an anion exchange membrane (AEM) (AMI-7001) in a dual chamber MFC and compared its performance with Nafion 117, cation exchange membrane (CEM) (CMI-7000) and Ultrafitration membranes (UFMs) with different molecular weight cut offs [14]. Among various membranes, AEM showed maximum performance, high values of power density (610 mW m^{-2}) and CE (72%) due to the presence of proton carriers such as phosphate anions which lowered internal resistance and made proton transfer easier. It seems as if AEM maintained a charge balance by redistribution of phosphate ions across the membrane. Rozendal *et al*. found that AEM maintains pH gradient between the two chambers more effectively than CEM as it allows the free movement of anions from cathode to anode and subsequently the potential loss by pH gradient is less in AEM.[15] One major drawback with CEM is that the cations other than protons pass through it freely and get precipitated on the cathode jeopardizing the performance. Mo *et al.* reported that AEM in an MFC may help stable power generation with reduced membrane resistance due to small cation precipitation.[16] Rozendal *et al*. used AEM (Fumasep®) in an MEC operated with wastewater and obtained the best hydrogen production efficiency.[17]

Though AEM eliminates pH splitting issues effectively, the fact that it favours substrate crossover, is certainly a setback.[18] This may encourage formation of biofilm on cathode surface curtailing the overall performance.[19, 20] Donning the role of a physical barrier for ion transfer from the anode to the cathode, the biofilm not only increases the pH gradient between the two chambers of the MFC but also defers the bacterial growth leading to poor performance.[21,22] An optimum performance necessitates the replacement of the fouled membranes with new membranes, which escalates operational cost. [22]

With the onset of nanotechnology in recent times, using novel nanocomposite materials like nanoparticles, carbon nanotubes and graphene as AEMs has borne fruitful results.[23–25] Past studies drive home the point that inclusion of functions nanofillers into an

AEM in need an improved ionic conductivity, mechanical stability and selectivity which eventually boosts up the performance of alkaline anion exchange fuel cells (AEFCs).[25, 26] Graphene oxide (GO) is a distinguished nanofiller in many ways because of its large surface area, hydrophilic nature, electronic insulation and good mechanical stability.[27, 28] The presence of significant amount of oxygen containing groups on the surface of GO makes it easily functionalizable using strong proton (or hydroxyl) exchange groups either by covalent or non-covalent bonding.[29, 30] It was found that Poly (diallyldimethylammonium) chloride (PDDA), a water soluble and chemically stable polyelectrolyte with excellent OH^- conductivity, can be used as a charge carrier in GO systems.[31] PDDA is a positively charged polymer due to the presence of amino groups. Therefore, negatively charged GO sheets can be strongly attracted by PDDA through electrostatic interaction. In addition, between GO sheets and PDDA chains can form multiple hydrogen bonds and GO sheets can self-assemble through π–π stacking interaction, also increasing the bonding force among GO sheets.[32]

In view of the above, the first objective of the present work is to functionalize GO sheets with PDDA by physical adsorption and then disperse it into the QPSU solution with the motive of increasing the density of anion exchange sites. Various FGO ratios were taken into consideration to ascertain the optimal conditions for fabricating the membranes. The second objective is to improve the antibacterial property as well as compatibility between the fillers and the polymer networks. The third and last objective is to analyze the effect of filler content on the properties of a nocomposites membranes as AEMs for its use in long term MFC applications.

2 Experimental

2.1 Materials

Poly sulfone and N-methyl-2-pyrrolidinone were purchased from Sigma Aldrich. Graphite (Alfa Esar) was used to prepare graphene oxide for modification of a QPSU membrane. Nitric acid, sulphuric acid, potassium permanganate and hydrogen peroxide were purchased from SRL chemicals, Mumbay, India. PTFE binder, platinum, iso propyl alcohol, sodium acetate, sodium dihydrogen phosphate, disodium phosphate, ammonium chloride, potassium chloride, magnesium sulphate, calcium chloride, metals, vitamins (Sigma Aldrich) were obtained commercially and used as received without further purification. Other chemicals like chloroform, methanol, triethylamine, dimethylformamide, paraformaldehyde, chlorotrimethylsilane and stannic chloride were purchased from Sisco Research Laboratory Pvt. Ltd, Mumbai, India. Vulcan XC-72 (20 % of Platinum in carbon support) and platinum on carbon were purchased from Arora Mathey Pvt. Ltd and the carbon cloth was obtained from Cobat carbon Inc. The commercial anion exchange membrane AMI 7001 purshased from membranes international Inc., USA.

2. 2 Synthesis of graphene oxide (GO)

Hummer's method is mostly used to synthesize Graphene oxide (GO) from graphite powder.[33] In the typical synthesis, 1 g of graphite with 0.5 g of sodium nitrate were mixed together and further 23 mL of conc. sulphuric acid was added along with it under constant stirring. Overheating and explosion were avoided by keeping the mixture at a temperature below 10 °C. After the addition of 3 g of potassium permanganate, the mixture was stirred vigorously at 35 °C for 12 h. The resulting solution was treated with 5ml of 30% hydrogen peroxide solution and washed thoroughly with hydrochloric acid alongwith water. Further, it was filtered and dried.

2.3 Preparation of quaternized polysulphone (QPSU) anion exchange membrane

2.3.1 Chloromethylation of poly sulphone

5 g polysulphone was dissolved in 75 mL chloroform at 70 °C to form a solution. After complete dissolution of polymer, a mixture of paraformaldehyde (3.4 g) and chlorotrimethylsilane (14.7 mL) was added as the chloromethylating agent with constant stirring, 5% (by weight, of polymer) of stannous chloride was added to the above mixture with stirring at 70 °C and allowed to react for 18 h. Afterwards the polymer was precipitated in methanol for removing the catalyst and solvent. Prior to drying, it was washed with methanol and de-ionized water several times.

2.3.2 Quaternization of poly sulphone

The chloromethylated polymer was dissolved in N, N dimethyl formamide (DMF), and poured into a round bottomed flask and a required quantity of triethylamine was slowly added. Then it was stirred at 70 °C for 20 h. After drying, the residue was dissolved in dimethyl formamide to get rid of excess and unreacted reagents and then precipitating using methanol. Then the ionomer was dried and dissolved in N-methyl-2-pyrrolidinone (NMP) solvent and the membrane was obtained using solution casting method and dried 60 °C for 24 h under vacuum oven.

2.3.3 Alkalization of poly sulphone

The obtained (quaternized) membrane was soaked in a 1.0 M aqueous potassium hydroxide solution at 30 °C temperature for 24 h. The alkalized membrane was then washed with de-ionized water several times and soaked in de-ionized water with numerous washings for 24 h prior to performance.

The ion exchange capacity (IEC), hydroxyl conductivity, water absorption percentage, oxygen and substrate crossover and thickness of the membranes were determined and the obtained values are tabulated (Table 1).

Table 1 Comparison of different Wt.% QPSU/FGO nanocomposites, QPSU and AMI-7001 membranes

2.3.4. Preparation of PDDA-functionalized graphene oxide (FGO)

Graphene oxide sheets were functionalized with PDDA by non covalent bonding. Suitable amounts of 1wt.% GO and 20wt.% PDDA aqueous solutions were mixed under stirring at 30 °C for 24 h. Then, the mixture was centrifuged at 4000 RPM for 15 min. The precipitate was then washed with distilled water to remove the excess PDDA. Finally, FGO was dried in an oven at 60 °C for 12 h.

2.3.5 Fabrication of QPSU/FGO nanocomposite AEMs

QPSU ionomer solutions were prepared using NMP as a solvent. Then appropriate amounts of FGO (0.5, 1.0, and 2.0 wt.%) were dispersed in QPSU solutions by sonication and stirred for 2 h. The required nanocomposite membranes were prepared by solvent casting method. The dried membranes were ion-exchanged in 1M KOH solutions.

2.4 Characterization of membranes

2.4.1 Structural characterization of membranes

2.4.1.1 Proton NMR spectroscopy

The chemical structure of the PSU, CMPSU and QPSU were investigated by ^{1}H NMR Bruker Advance 500 MHz multinuclear FT-NMR spectrometer with $CDCl_3$ as the solvent.

2.4.1.2 Infra- red spectroscopy

The chemical structures of GO, FGO and QPSU/FGO membranes were confirmed with FTIR Alpha Bruker spectrometer in transmittance mode. A spectral range varying from 500 to 4000 cm^{-1} at a resolution of 4 cm^{-1} was assigned for these studies. The scan rate was kept as 100 scans per sample.

2.4.1.3 Raman spectroscopy

The main features in the Raman spectra of graphitic carbon-based materials are the G and D peaks and their overtones. Raman spectra were obtained using Lab RAM HR 800 (Horiba Jobin Yvon, France). Initially, Raman spectrometer was calibrated with carbon tetra chloride (CCl_4) for standard peaks at 218 cm^{-1}, 314 cm^{-1} and 459 cm^{-1}. Instrument control, data collection, and data pre-processing were performed using Lab spec software as provided by the instrument manufacturer (Horiba Jobin Yvon, Rue de Lille, France). The samples were mounted on a glass substrate and a laser beam was focussed on the centre of sample surface.

2.4.1.4 X-ray photoelectron spectroscopy

The chemical state and composition of the products were analyzed by X-ray photoelectron spectroscopy (XPS, K-Alpha, Thermo Scientific, UK), equipped with a mono chromator Al Kα source at a spot size of 400 μm and pass energy of 30 eV. The peaks were fitted and analyzed using Thermo Avantage software.

2.4.1.5 X-ray diffraction (XRD)

X-ray diffraction (XRD) is a technique used to identify the crystalline and amorphous nature of materials. In the present study, XRD spectra of the membrane samples were recorded using an X'Pert Pro diffractometer (PANalytical). The scanning angle was 1–80° with a scanning rate of 2 per min.

2.4.2 Topological characterization of membraness

2.4.2.1 SEM-EDAX analysis

The surface morphology of the GO, QPSU, QPSU/FGO nanocomposite membranes were studied using VEGA3 TESCAN Scanning Electron Microscope (SEM). Prior to SEM analysis, the samples were dried and then coated with gold by sputtering. High resolution scanning electron microscope (HR-SEM JEM-5600LV) with EDAX technique (Oxford Instruments X-ray Microanalysis) were used to analyze the elemental distribution on PDDA funtionalized GO.

2.4.3 Electrochemical measurements

2.4.3.1 Membrane ionic conductivity

A specimen of fully hydrated membrane was placed in a custom-made conductivity cell (0.62 cm^2) and A.C. impedance was measured in a galvanostatic mode (Bio logic VSP, France) over a frequency range of 100 Hz to 1 MHz under 10 mV oscillation potential. The conductivity values were calculated using equation (2)

$$\sigma = L/RA \qquad (1)$$

Where σ is the proton conductivity of the membrane in S cm^{-1}, L is the membrane thickness in cm, R is the membrane resistance in Ohm and A is the area of cross section of the electrode in cm^2.

2.4.3.2 Internal resistance of the MFC measurement

Internal resistance (Rin) of the reactors with different membranes was measured using the anode as the working electrode and the cathode as the counter and reference electrode.

Impedance measurements were conducted at the open circuit voltage (OCV) over a frequency range of 0.1 Hz to 1.0 KHz.

2.4.4 Physiochemical characterization

2.4.4.1 Hydrophilicity and water absorbance ratio of membranes

For contact angle measurement, the samples were fixed flat on a glass slide using double side tape and dried. Water droplets of a constant volume were made to fall on the ssurface of membrane by a contact angle System OCA (Data physics).

The Water Absorbance Ratio (WA) was calculated according to WA (%) = (Wwet-Wdry) / Wdry × 100%, where wwet and wdry represent the weight of dried membrane and membrane soaked in water at 30°C for 24 h, respectively.

2.4.4.2 Ion exchange capacity and thickness of membranes

The alkalized polymer membrane was equilibrated with 50 mL of 0.01M HCl aqueous solution for 24 h, followed by back titration method.[34] The IEC of the anion-exchange membrane was calculated based on the formula:

$$IEC = (Mo - Mt)/Wd$$

Where *M*o is the moles of HCl added originally and *M*t is the moles of HCl or equivalent to the moles of potassium hydroxide consumed during back titration and *W*d is the wt. of the dried membrane. AEM was obtained by casting the preweighed QPSU ionomer dissolved in DMF solution onto a glass plate with the thickness of the membrane restricted to 25 -30 µm.

2.4.5 Anti -bacteria and anti-adhesion tests

Anti-adhesion and anti-bacteria tests on membranes were conducted with mixed culture bacteria from an activated sludge in the vicinity (Anna University, Chennai-India). A flask with 30 mL of nutrient broth (NB) was placed in a 37 °C incubator shaker (India labbs) for 24 h to obtain the overnight phase of the bacteria. Then 1mL of culture was pipetted from the overnight phase into another flask with freshly prepared 30 mL of NB. The mixture was again placed in a 37 °C incubator shaker for another 5 h till it reaches the log phase of the bacteria. This step was necessitated as the log phase is generally endowed with more activity and viability than other phases.

Anti-bacteria tests were carried out for QPSU, QPSU/GO and QPSU/FGO membranes. About 100 mL of the prepared culture suspension was pipetted into an agar plate and then spread throughout the surface. A disc of each membrane was placed on the agar surface so that it covers an area in the middle of the plate. This was repeated for all membranes. These agar plates were then placed in an incubator at 37 ◦C for 24 h following which the agar plates were visually examined for the bacteria colonies.

2.4.6 MFC construction and operation

The fabricated MFC consisted of an acrylic cylindrical chamber 4 cm long and 3 cm in diameter (empty bed volume of 28 mL); anode surface area per volume of 12.5 m^2 m^3 separated with a QPSU anion exchange membrane (projected area of 12.5 cm^2).[35] The carbon cloth used as anode electrode was made wet proof with 30 % PTFE and subsequently coated with carbon bilayer 3 g cm^{-2} of Vulcan XC 72. The carbon bilayer slurry was prepared by mixing 70 wt% Vulcan XC- 72 and 30 wt% PTFE binder solution adding adequate double distilled water and isopropyl alcohol. The black mixture was ultra sonicated for 30 min and then coated using a brush on carbon cloth used as both anode and cathode. Then the cloth was

dried in a vacuum oven at 100 °C for 2 h and kept in muffle furnace at 350 °C for 6 h. Then cathode was fabricated using carbon supported platinum black of 0.5 mg cm^{-2} by a similar procedure, where double distilled water and isopropyl alcohol were added with respect to the wt.% of carbon on platinum catalyst.[36]

All MFCs (QPSU, QPSU/GO, QPSU/FGO and AMI-7001) were inoculated with the culture from an anode chamber of three years operated MFC reactor, which was originally inoculated with the domestic wastewater collected from Anna University sewage treatment plant (Chennai, India). The anode was filled with a solution prepared on the basis of COD containing sodium acetate substrate at a concentration of 1 g L^{-1}, in a phosphate buffered nutrient medium (PBM) containing NH_4Cl 0.31 g L^{-1}, $NaH_2PO_4.H_2O$ 4.97 g L^{-1},$Na_2HPO_4.H_2O$ 2.75 g L^{-1}, KCl 0.13 g L^{-1}, minerals (12.5 mL) and vitamins (12.5 mL). At the end of every cycle of operation, the voltage falls down below 20 mV and the anode chamber needs to be refilled with fresh solution to bring it back to steady state again. All tests were conducted in a room controlled with 30 °C temperature.

2.4.7 Analytical measurements and calculations

Voltage was measured using a digital multimeter (Model 702, Metravi, India). The external circuit was completed with a fixed load (resistance) of 1000 Ω. A set of variable resistors in the range 100 Ω-1000 Ω were used to determine the power generation as a function of load. Current (I) and power P (P =IV) were calculated by standard procedure[37].

The Columbic Efficiency (CE) was calculated using the following equation.

$$CE = Cp / CT \times 100\ \% \qquad (2)$$

Where, Cp is the total charge (in coulomb) calculated by integrating the current over time. C_T is the theoretical amount of charge (in coulomb) that can be produced from acetate and is calculated as;

$$C_T = \frac{FbSv}{M} \quad (3)$$

Where, F is Faraday's constant (96485 C/mol of substrate), b is the number of electrons produced per mol of substrate (acetate) (b=8), S is the substrate (acetate) concentration in g L^{-1}, v is the liquid volume in mL and M is the molecular weight of the substrate (acetate) (M = 82.3 g).[38]

3 Results and discussion

3.1 Proton NMR spectroscopy

The ^{1}H-NMR spectra of PSU, CMPSU and QPSU are shown in Fig. 1. (C) PSU showed chemical shifts of 7.27–7.8 (multi Hs on phenyl groups) and 1.73 (CH_3). The characteristic peak of $-CH_2Cl$ corresponding to the newly formed chloromethyl group could be seen at 4.6 ppm (Fig. 1. (B)). This peak confirms the successful preparation of the chloromethylated poly sulphone.[39] whereas in Fig. 1. (A) QPSU disappearance of 4.6 ppm and appearance of new chemical shift at 2.72 ppm (CH_3 linked to N) confirmed the formation of the quaternized poly sulphone .

Fig. 1 Proton NMR spectra of (A) QPSU (B) CMPSU and (C) PSU

3.2 Fourier transform infra-red spectroscopy

The appearance of a broad peak between 3000 –3700 cm^{-1} in the high frequency range and a sharp peak at 1635 cm^{-1} correspond to the stretching and bending vibration of OH molecules adsorbed on graphene oxide, confirming the sample's strong hydrophilicity

(Fig.2). The stretching vibration of C=C of carboxylic acid is represented by the peak at 1630 cm^{-1}, and the same for C=O of carbonyl groups by a peak at 1740 cm^{-1}. The two absorption peaks at 2930 cm^{-1} and 2850 cm^{-1} are assigned to the symmetric and anti-symmetric stretching vibrations of CH_2.[40] The absorption peak at 1385 cm^{-1} denotes the stretching vibration of C–O of carboxylic acid and the one at 1110 cm^{-1} implies to C–OH of alcohol. The presence of PDDA on the GO sheets is established by the presence of two additional bands at 2102 and 2918 cm^{-1} as well as by the absence of bands at 1745 and 1053 cm^{-1}. The most probable reason may be the strong interaction between the oxygen-containing groups in the GO and PDDA.

Fig. 2 FT-IR spectra of GO, FGO and QPSU/FGO

3.3 Raman spectroscopy

The first-order G peak, at 1580 cm^{-1} may represent the optical E_2g phonons at the Brillouin zone center due to the bond stretching of sp^2 carbon pairs in both rings and chains. The first-order D peak at 1350 cm^{-1}, whose intensity is a measure of degree of disorder, may be due to breathing mode of aromatic rings at the behest of defects in the sample[41,42] (fig. 3). The peak at 1350 cm^{-1} usually represents the QPSU membrane but a relatively broad one at 1588 cm^{-1}, arising from the structural imperfections due to epoxide and hydroxyl groups, confirms the presence of FGO on QPSU membrane.[43–44]

Fig. 3 Raman spectra of GO, FGO and QPSU/FGO

3.4 Scanning Electron Microscopy

Fig.4 (I) shows the synthesis of GO with different scale bars. The ultra thin and homogeneous structure of GO films with distinguishable edges including sporadic bends and folds are predominantly visible. From fig. 4 (II), it is clear that among QPSU, QPSU/GO and QPSU/FGO membranes with different wt.%, only the QPSU/FGO-2.0 % membrane appears

to have a rough morphology due to agglomeration of FGO content but for others the morphology was found to be smooth and compact. From Fig. 5(A), it is shown that the Cl (13.23 wt%) element is present on the surface of the functionalized GO, which means that the PDDA containing chloride ion (Cl) has properly condensed with the GO. However, Nitrogen element was not detected in the SEM-EDAX due to higher accelerating voltage of SEM that lowers the efficiency to ionize the nitrogen. When accelerating voltage is lowered spectrum doesn't appear because EDAX detector does not receive enough photons.

The stability of the immobilized PDDA on GO (FGO) was evaluated with a dynamic leaching system. An amount of prepared FGO was put into a sealed flask filled with approximately 50 ml of DI water. After magnetic stirring for 24 h at 300 rpm, and after drying the samples were again examined for SEM-EDAX to understand the leaching out of PDDA from FGO and we found the presence of 11.82 wt.% of chloride ion 5 (B) of PDDA over GO, which implies that the content of PDDA still remains intact with FGO due to dipole-dipole interactions and hydrogen bonding.

Fig. 4 (I). SEM images of synthesized graphene Oxide (A-D), Fig. 4 (II). SEM images of membrane surface (A) QPSU, (B) QPSU/FGO-0.5 wt.%, (C) QPSU/FGO-1.0 wt.%, (D) QPSU/FGO-2.0 wt. %.

Fig. 5 EDAX analysis of FGO (A) FGO, (B) Water dispersed FGO

3.5 X-ray Photoelectron Spectroscopy

XPS analysis is a versatile tool for verifying the ratio of constituent elements in a compound. XPS spectrum at 0-800 eV shows that the elements Carbon and Oxygen, the main species found in GO, are in the ratio of 1:2 (Fig. 6A). A high degree of oxidation with four different carbon environments of sp^2-C (284.3 eV), C–O (285.1 eV), C=O (286.9 eV) and COOH (288.4 eV) is proved by C1s XPS of prepared GO (Fig. 6B). The peaks at 531.6 eV

and 532.5 eV are attributed to the C=O and C-OH bonds respectively in O1s XPS of GO(Fig. 6C). The peak at 533.4 eV may be due to absorption by OH (or H_2O) species during fabrication, endorsing the presence of oxygen functional groups.[45]

Fig. 6 XPS spectra of GO (A) survey spectra (B) C 1s and (C) O 1s

3.6 X-ray Diffraction

XRD analysis of GO, FGO, QPSU and QPSU/FGO were shown in fig. 7. A high intensity peak at $2\theta = 10.6°$ indicates the crystalline nature of GO.[42] The absence of such a strong peak in the case of FGO suggests the amorphous nature of FGO when functionalized with PDDA. A broad peak at $2\theta = 19.7°$ shows the presence of QPSU membrane, a typical semicrystalline polymer. The crystallinity of the membranes increases with FGO content as FGO may be the crystallization nucleus for QPSU. A better ionic conductivity and hence the performance depends on the mixing of QPSU and FGO in the appropriate ratio.[46]

Fig. 7 XRD spectra of GO, FGO, QPSU/FGO and QPSU

3.7 Effect of membrane modification on anti-adhesion property

Membrane modification plays a vital role in determining the hydrophilicity and bacterial anti-adhesion tests. Except the QPSU/GO (2.0 wt.%), all other membranes, ie, QPSU, QPSU/GO and QPSU/FGO showed better performance due to enhanced hydrophilicity. It is clear from Table 1 that GO content has a reciprocal relationship with contact angle. The SEM images in Fig. 8 (I) confirm that after a 4 h contact with the bacteria culture, QPSU and AMI-7001 only were found with substantial amount of bacteria on the surface owing to high surface hydrophobicity. The functional groups such as carboxyl, epoxy and hydroxyl present on the basal planes and edges of GO may be the source for augmented hydrophilicity.[47, 48] A high infiltration of water due to enhanced hydrophilicity reduces the interfacial energy between membrane surface and water and weakens biofouling.[49, 50] As a

result, the microorganisms like bacteria and biomolecules like proteins with hydrophobic nature are forbidden from adhering to the membrane surface.[51, 52] Another significant point is that hydrophilic surfaces are thermodynamically less advantageous due to low interfacial energy.[53]

Fig. 8 (I) SEM images of membrane surface for anti adhesive property (A) QPSU, (B) QPSU/FGO-0.5 wt.%, (C) QPSU/FGO-1.0 wt.%, (D) AMI 7001, Fig. 8 (II) Photographic images of anti bacterial property (A) QPSU, (B) QPSU/GO (C) QPSU/FGO-0.5 Wt.% (D) QPSU/FGO-1.0 Wt.%.

3.8 Effect of membrane modification on anti-bacteria property

In an agar plate, mixed culture was spread on the agar plate. A small portion in the middle was covered with a membrane disc. The plates were examined after a time gap of 24 h for ascertaining bacterial growth (Fig. 8 (II)). Colonies of bacteria were found only in QPSU and QPSU/GO but not in QPSU/FGO. The presence of quaternary ammonium moieties with high charge density and antimicrobial activity in QPSU/FGO may be attributed for this remarkable observation.[54] It is supposed that compounds with quaternary ammonium groups destroy the bacterial cell and release K^+ ions and other cytoplasmic constituents resulting in immediate death of the bacterial cell.[55] So the destruction of the bacteria is beneficial in two ways, viz, reducing the internal resistance and increasing the ion transfer.[56] So the final conclusion is that modification of QPSU membrane with PDDA on GO nanoparticles accelerates MFC performance due to reduced biofouling. Hence QPSU/FGO based AEM could be a potential membrane for long term application in MFC.

3.9 MFC performance

All five MFCs were performed under similar conditions. For stabilization, MFCs were allowed to run without any external load initially and data were recorded. Within 2 days

of biofilm activation, random fluctuations were observed in anode and cathode potentials, with an average of 350 mV and +0.185 V (with Ag/AgCl Ref. Electrode) in all MFCs (data not shown). These fluctuations were considered as part of system acclimatization where a gradual increment in OCV (open circuit voltage) was observed within 6 days in all MFCs. MFC with QPSU/FGO-1.0 % membrane showed frequent OCV rise within 10 days, but lower increment in OCV was observed with other four MFCs. A maximum potential of 701 ± 20 mV, 756 ± 30 mV, 731± 18 mV, 723 ± 28 mV and 701 ± 20 mV was observed with QPSU/FGO-0.5%, QPSU/FGO-1.0%, QPSU/FGO-2.0%, QPSU and AMI-7001 respectively in 60 days run (Fig. 9). The increased OCV and current in QPSU/FGO-1.0% may be a consequence of the optimal concentration of FGO groups on PDDA functionalization which indicates its efficacy as AEM. In the case of QPSU/FGO-2.0%, its lowest OCV and current outputs show that it is inferior to QPSU/FGO-1.0% and QPSU/FGO-0.5% in ion conduction. In this case, a lower conductivity may be due to agglomeration caused by increased concentration. All these results substantiate the fact that adding FGO on QPSU membrane enhances its potential as AEM. QPSU/FGO1.0% recorded the highest efficiency with maximum power and current density of 1036 ±15 mW m^{-2} and 2880 ± 70 mA m^{-2} respectively. On comparison, QPSU/FGO0.5% (945 ± 8 mW m^{-2} and 2780 ± 48 mA m^{2}), QPSU/FGO 2.0% (874 ± 4 mW m^{-2} and 2300 ± 27 mA m^{-2}), QPSU (805 ± 2 mW m^{-2} and 2120 ± 13 mA m^{-2}) and AMI 7001(576 mW m^{-2} and 1800 mA m^{-2}) showed relatively lower values. These findings make QPSU/FGO-1.0 % membrane an exemplary over others due to its higher IEC, increased water uptake, and enhanced conductivity. However, an additional test was performed using PSU (without quaternization) to find out the effect of excess adsorbed KOH and the obtained IEC value of PSU was found to be 0.01 meq g^{-1}. Besides, an increase in the hydrophilic fraction of the membrane, the isolated hydrophilic domains will expand and intertwine upon hydration for opening new channels for ion transportation. It is a

well known fact that the ionic conductivity of a membrane is directly influenced by the dimensions of the functional groups and absorbed water molecules.[57] The fact that membranes with high filler content exhibit high water uptake exactly fits FGO which is incidentally a hydrophilic material with high surface area. In fact, QPSU/FGO-1.0% recorded a whopping 44.4% more power output than the commercially available membrane AMI-7001, 22.2% more than QPSU and 15.6% more than QPSU/FGO-2.0% and 8.7% more in the case of QPSU/FGO-0.5%.

Fig. 9 Power generation during MFC operation with QPSU/FGO-0.5 wt.%, QPSU/FGO-1.0 wt.%, QPSU/FGO-2.0 wt.%, QPSU and AMI-7001.

3.10 Electrochemical impedance spectroscopy (EIS) analysis

The cell resistances from the EIS graphs were plotted for MFC with QPSU/FGO-0.5 %, QPSU/FGO-1.0%, QPSU/FGO-2.0%, QPSU and AMI-7001 respectively (Fig. 10). Minimal resistance was found in case of QPSU/FGO-1.0% than other MFCs. The internal resistance of the whole cell was segmented into various component resistances, viz activation resistance, ohmic resistance, electrode resistance, membrane resistance and concentration resistance etc.[58, 59] The ohmic resistance as calculated from the EIS graphs were found to be 11.6 Ω for QPSU/FGO-1.0%, 18.1 Ω for QPSU/FGO-0.5%, 22.2 Ω for QPSU/FGO-2.0%, 24.8 Ω for QPSU and 32.6 Ω for AMI-7001. The least ohmic resistance in the case of QPSU/FGO-1.0% is the reason behind its improved ionic conduction among other membranes. But a high value of ohmic resistance measured for MFC with QPSU and AMI-7001 shows their inherent high resistance to charge transfer across the membranes. This was an expected result, as the used pure QPSU and AMI-7001 were hydrophobic and having minimal ionic conduction. The data clearly show minimal ionic hindrance in case of QPSU/FGO-1.0% than other membranes. It is believed that an increase in FGO content (except for QPSU/FGO-2.0%) enhances membrane polarity resulting in high transverse ionic

conduction. The increased IEC and proton conductivity in QPSU/FGO-1.0%, allows more passage of ions than other membranes, resulted in increased MFC efficiency with minimal impedance.

Fig. 10 Nyquist representation of the electrochemical impedance of QPSU/FGO-0.5 wt.%, QPSU/FGO-1.0 wt.%, QPSU/FGO-2.0 wt.%, QPSU and AMI-7001.

4 Conclusion

In summary, an attempt has been made to prepare novel nanocomposite AEMs containing QPSU membrane with modified FGO. A detailed investigations have been done on QPSU/FGO nanocomposites with pure QPSU and commercially available AMI-7001 membranes. Among the combinations, QPSU/FGO-1.0% shows excellent performance with higher power and current densities. Out of two familiar anti biofouling measures, the anti adhesive approach prevents the attachment of bacteria on a membrane, whereas anti-microbial approach kills bacteria already present on the membrane. To the best of our knowledge, involving both anti-adhesive and anti-microbial approach is one of the best innovative methods to control and minimize membrane biofouling.

Acknowledgement

The authors would like to thank Department of Science and Technology-Alternate Fuel Technology for funding the project vide the sanction letter No. DST/TSG/AF/2010/09 and Department of Mechanical Engineering, Anna University, Chennai, India for providing necessary laboratory facilities.

References

1. L.T. Angenent, K. Karim, M.H. Al-Dahhan, B.A. Wrenn, R. Domíguez-Espinosa*, Trends Biotechnol.* 2004, 22, 477–485.

2. S. Venkata Mohan, S. Veer Raghuvulu, S. Srikanth, P.N. Sarma, *Curr. Sci.* 2007, 92, 1720–1726.

3. D.R. Bond, D. Lovley, *Appl Environ Microbiol.*2005,71 ,2186-2189.

4. S. Venkata Mohan, S. Veer Raghavulu, P.N. Sarma, *Biosens. Bioelectron*. 2008, 24, 41–47.

5. W.-W. Li, G.-P. Sheng, X.-W. Liu, H.-Q. Yu, *Bioresour. Technol.* 2011 ,102, 244-252.

6. S. Oh, B. Min, B.E. Logan, *Environ. Sci. Technol.* 2004, 38, 4900-4904.

7. K.J. Chae, M. Choi, F.F. Ajayi, W. Park, I.S. Chang, I.S. Kim, *Energy & Fuel,* 2007, 22, 169-172.

8. J. Xu, G.-P. Sheng, H.-W. Luo, W.-W. Li, L.-F. Wang, H.-Q. Yu, *Water Research.* 2012, 46, 1817-1824.

9. M. M. Ghangrekar, V.B. Shinde, *Bioresour. Technol.* 2007, 98, 2879-2885.

10. J.R. Kim, S. Cheng, S.-E. Oh, B.E. Logan, *Environ. Sci. Technol.* 2007, 41,1004-1009.

11. X. Tang, K. Guo, H. Li, Z. Du, J. Tian, *Biochemical Engineering Journal.* 2010,52, 194-198.

12. X. Zhang, S. Cheng, X. Wang, X. Huang, B.E. Logan, *Environ. Sci. Technol.* 2009, 43, 8456-8461.

13. A. Rinaldi, B. Mecheri, V. Garavaglia, S. Licoccia, P. Di Nardo, E. Traversa*, Energy Environ. Sci.* 2008, 1, 417-429.

14. J.R. Kim, S. Cheng, S.E. Oh, B.E. Logan, *Environ. Sci. Technol.* 2007, 41, 1004–1009.

15. R.A. Rozendal, H.V.M. Hamelersa, R.J. Molenkamp, C.J.N. Buisman, *Water Res.* 2007, 41, 1984–1994.

16. Y.Mo, P. Liang, X. Huang, H. Wang, X.Cao, *J Chem. Technol. Biotechnol.*2009, 84 1767–1772.

17. R.A Rozendal, T. Sleutels, H.V.M. Hamelers, C.J.N. Buisman, *Water Sci. Technol.* 2008, 57, 1757–1762.

18. S. Pandit, S. Ghosh, M.M.Ghangrekar, D. Das, *Int. J. Hydrogen Energy.* 2012, 37, 9383–9392.

19. K.J. Kim, K.J. Chae, M.J. Choi, E.T. Yang, M.H. Hwang, I.S. Kim. *Chem. Engg. J.* 2012, 218, 19–23.

20. J.D. Seader, H.J. Henley. New York: *Wiley*, 1998.

21. T.H. Choi, Y-B. Won, J-W. Lee, D.W. Shin, Y.M. Lee, M. Kim, *J. Power Sources.* 2012, 220, 269–79.

22. J. Xu, G.P. Sheng, H.W. Luo, W.W. Li, L.F. Wang, H.Q. Yu, *Water Research.* 2012, 46, 817–824.

23. P. Nonjola, M. Mathe, and R. Modibedi, *Int. J. Hydrogen Energy.* 2013,38, 5115-5121.

24. R. Vinodh, M. Purushothaman, D. Sangeetha, *Int. J. Hydrogen Energy.* 2011, 36, 722-729.

25. P. Leung, Q. Zhao, L. Zeng, and C. Zhang, *Electrochim. Acta,* 2013, 105, 584-592.

26. P. Leung, Q. Zhao, L. Zeng, and C. Zhang, *Electrochim. Acta,* 2013, 105, 584-592.

27. Y. Ye, M. Cheng, X. Xie, J. Rick, Y. Huang, F. Chang, and B. Hwang, *J. Power Sources.* 2013, 239, 424-432.

28. M. Gudarzi and F. Sharif, *Express Polym. Lett.* 2012,6, 1017-1031.

29. S. Wang, D. Yu, L. Dai, D. Chang, and J. Back, *ACS Nano.* 2011, 5, 6202-6209.

30. Y. Li, C. Deng, and M. Yang, *Sensor Actuat. B-Chem.* 2014,194, 51-58.

31. S. Pandit, S. Khilari, K. Bera, D. Pradhan, and D. Das, *Chem. Eng. J.* 2014, 257, 138-147.

32. X. Wang, Z. Liu, X. Ye, K. Hu, H. Zhong, J. Yu, M. Jin, Z. Guo, *Appl. Surf. Sci.* 2014, 308, 82–90.

33. S. Niyogi, E. Bekyarova, M. E. Itkis, J. L. McWilliams, M. A. Hamon, R. C. Haddon, *J. Am. Chem. Soc.* 2006, 128, 7720-7721.

34. G.-J. Hwang, H. Ohya, *J. Membr. Sci.* 1998, 140, 195–203.

35. O. Lefebvrea, Y. Shena, Z. Tana, A. Uzabiagaa, I. S. Changb, H. Y. Nga, *Bioresour. Technol.* 2011, 102 , 6291–6294.

36. S. Ayyaru, S. Dharmalingam, *Bioresour. Technol.* 2011, 102, 11167-11171.

37. R. J. Kim, B. Min, BE. Logan, *Appl. Microbiol. Biotechnol*. 2005,68, 23-30.

38. T.H.J.A. Sleutelsa, L. Darusb, H.V.M. Hamelersa, C.J.N. Buismana, *Bioresour. Technol*. 2011,102, 11172-11176.

39. M.R. Hibbs, M.A. Hickner, T.M. Alam, S.K. McIntyre, C.H. Fujimoto, C.J. Cornelius, *Chem. Mater.* 2008, 20, 2566-2573.

40. H. Guo, X. Wang, Q. Qian, F. Wang, X. Xia, *ACS Nano.* 2009,3, 2653-2659.

41. F. Tuinstra, J. L. Koenig, *J. Chem. Phys.* 1970, 53, 1126-1130.

42. A. C. Ferrari, J. Robertson, *Phys. Rev. B,* 2000, 61, 14095-14107.

43. C. Gómez-Navarro, R.T. Weitz, A. M. Bittner, M. Scolari, A. Mews, M. Burghard, K. Kern, *Nano Lett.* 2007, 7, 3499–3503.

44. D. Graf, F. Molitor, K. Ensslin, C. Stampfer, A. Jungen, C. Hierold, L. Wirtz, *Nano Lett.* 2007,7, 238–242.

45. C. Tao, J. Wang, S.Qin, Y. Lv, Y. Long, H. Zhua, Z. Jianga, *J. Mater. Chem., 2012,22, 24856-24861*.

46. D. Yang, A. Velamakanni, G. Bozoklu, S. Park, M. Stoller, R. D. Piner, S. Stankovich, I. Jung, D. A. Field, C. A. Ventrice *Jr. Carbon*, 47 2009 145–152.

47. E.D. Wang, T.S. Zhao, W.W. Yang. *Int J. Hydrogen Energy.* 2010,35, 2183-2189.

48. D.A. Dikin, S. Stankovich, E. J. Zimney, R. D. Piner, G. H. B. Dommett, G. Evmenenko, S. B. T. Nguyen, R. S. Ruoff, *Nature*. 2007,448, 457–460.

49. D.R. Dreyer, S. Park, C. W. Bielawski, R. S. Ruoff, *Chem. Soc. Rev.* 2009,39, 228–240.

50. P.Le-Clech, V. Chen, T. A. G. Fane, *J. Membr. Sci.* 2006, 284, 17–53.

51. S. Krishnan, C. J.Weinman, C. K. Ober, *J. Mater. Chem.* 2008, 18, 3405–3413.

52. M. Van Loosdrecht, W. Norde, A. Zehnder, *J. Biomater. Appl.* 1990,5, 91–106.

53. M. Van Loosdrecht, J. Lyklema, W. Norde, G. Schraa, A. Zehnder, *Appl. Environ. Microbiol.* 1987,53, 1898–1901.

54. I. Cakmak, Z. Ulukanli, M. Tuzcu, S. Karabuga, K. Genctav, *Eur. Polym. J.* 2004,40, 2373–2379.

55. T. Tashiro, *Macromol. Mater. Eng.* 2001,286, 63–87.

56. L.D. Melo, E.M. Mamizuka, A.M. Carmona-Ribeiro, *Langmuir.* 2010, 26, 12300–12306.

57. Q. Duana, S. Gea, C-Y. Wanga, *J. Power Sources.* 2013, 243, 773-778.

58. Z. He, F.Mansfeld, *Energy Environ Sci.* 2009,2, 215–219.

59. X. Li, X. Wang, Y. Zhang, N. Ding, Q. Zhou, *Appl. Energy.* 2014,123, 13–18.

Table.1. Comparison of different Wt.% QPSU/FGO nanocomposites, QPSU and AMI-7001 membranes

Membrane Type	**Thickness (μm)**	**Ionic conductivity (S cm^{-1})**	**Ion exchange capacity (meq g^{-1})**	**Water absorbance (%)**	**Contact angle (degree)**
QPSU/FGO-0.5 %	30	1.87×10^{-2}	1.42	42.56	73
QPSU/FGO-1.0 %	30	1.96×10^{-2}	1.45	43.34	64
QPSU/FGO-2.0 %	30	1.81×10^{-2}	1.37	55.59	59
QPSU/GO	30	1.83×10^{-2}	1.23	42.11	71
QPSU	30	1.80×10^{-2}	1.02	41.31	78
AMI-7001	450	1.72×10^{-2}	1.30	17.00	108

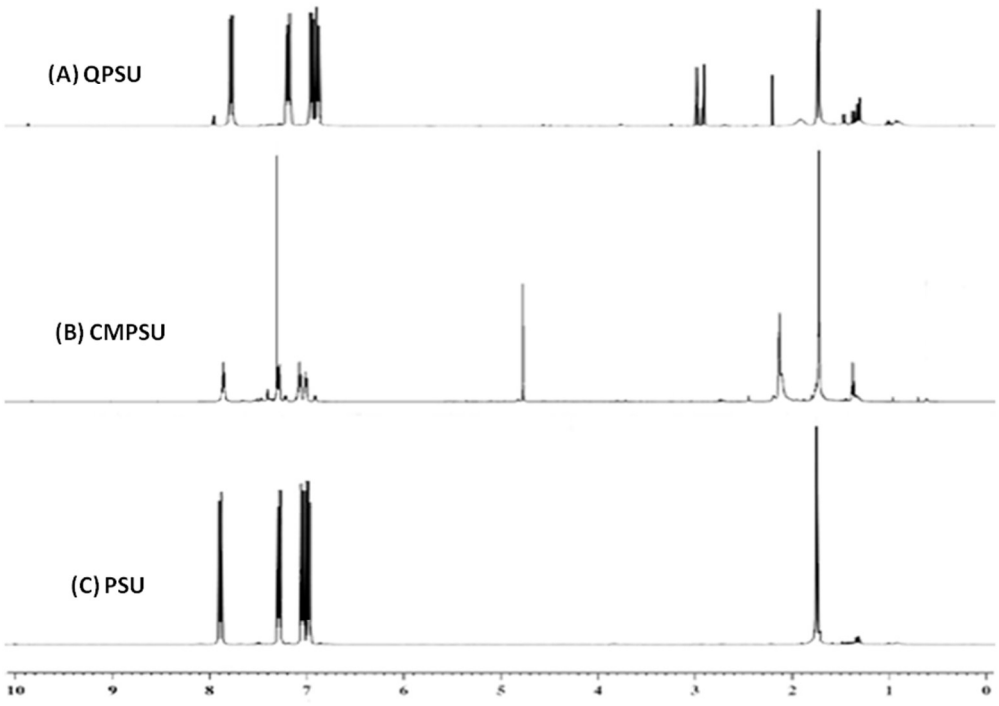

254x190mm (96 x 96 DPI)

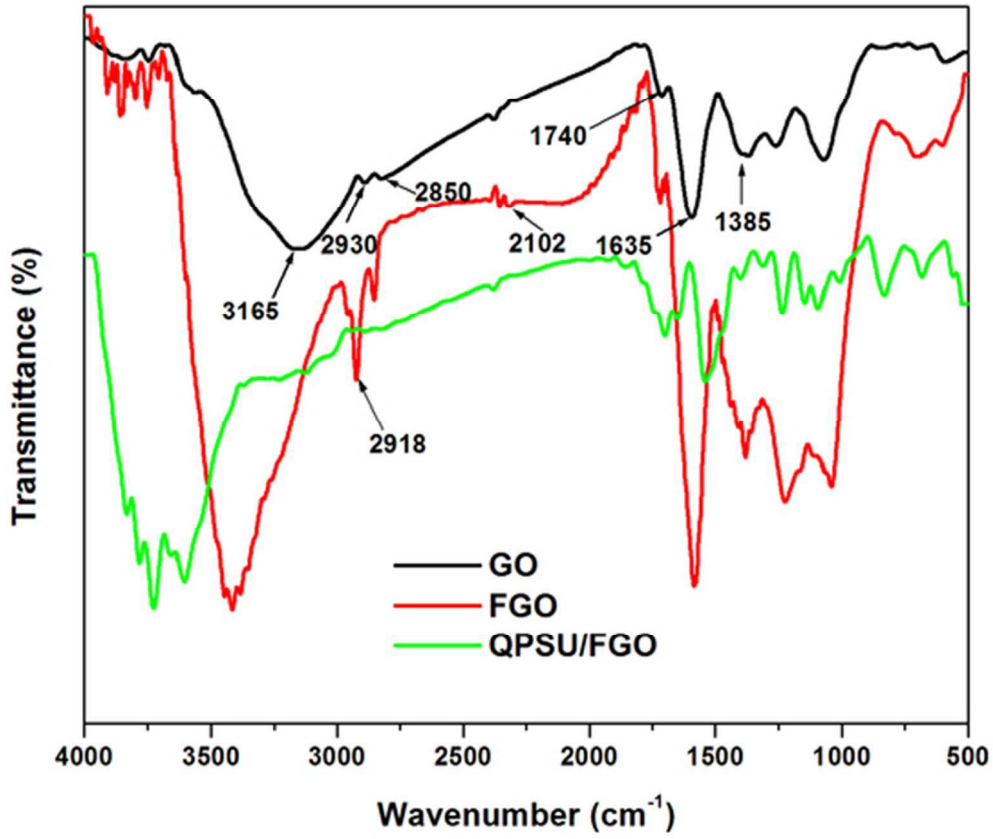

46x39mm (300 x 300 DPI)

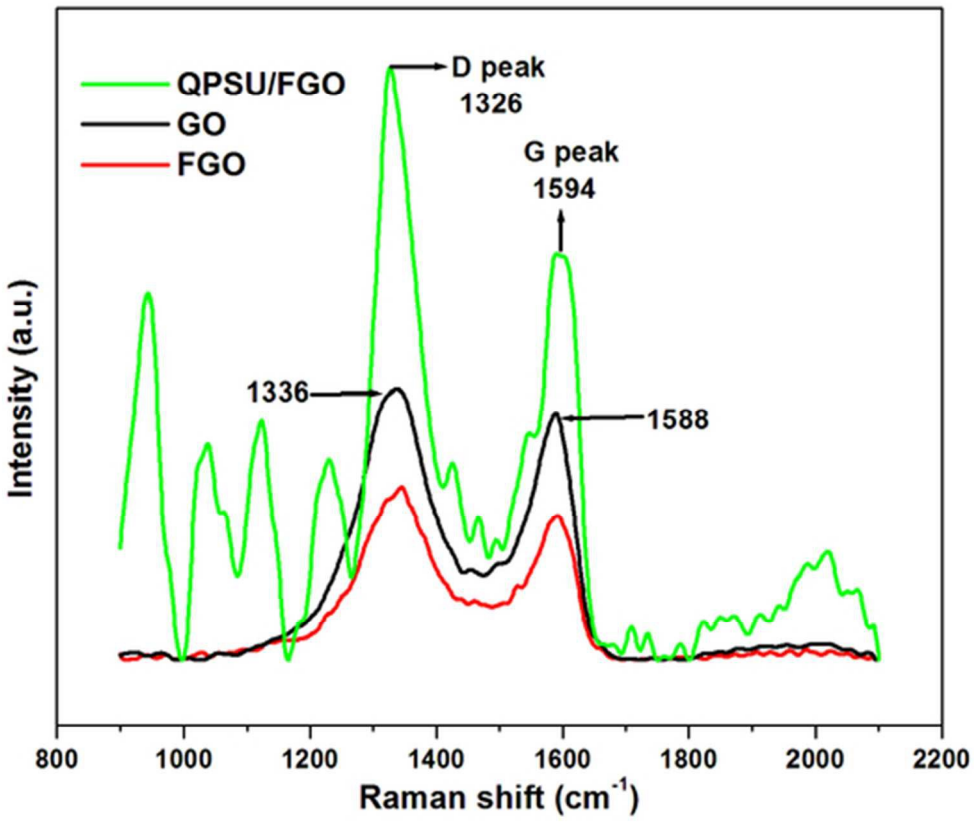

45x38mm (300 x 300 DPI)

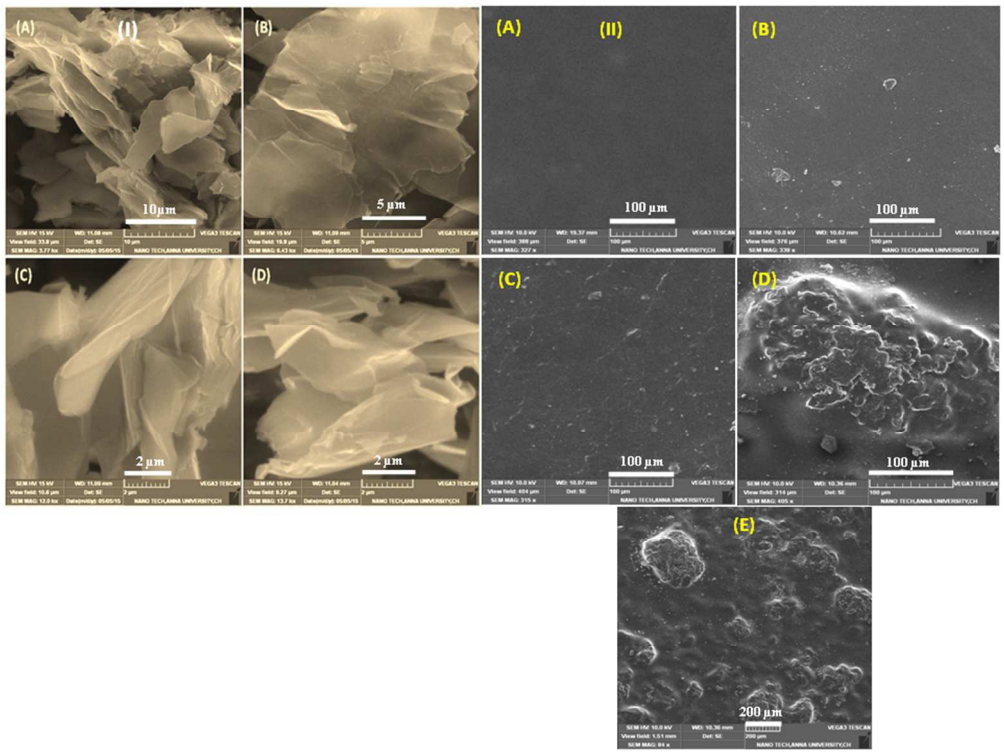

254x190mm (96 x 96 DPI)

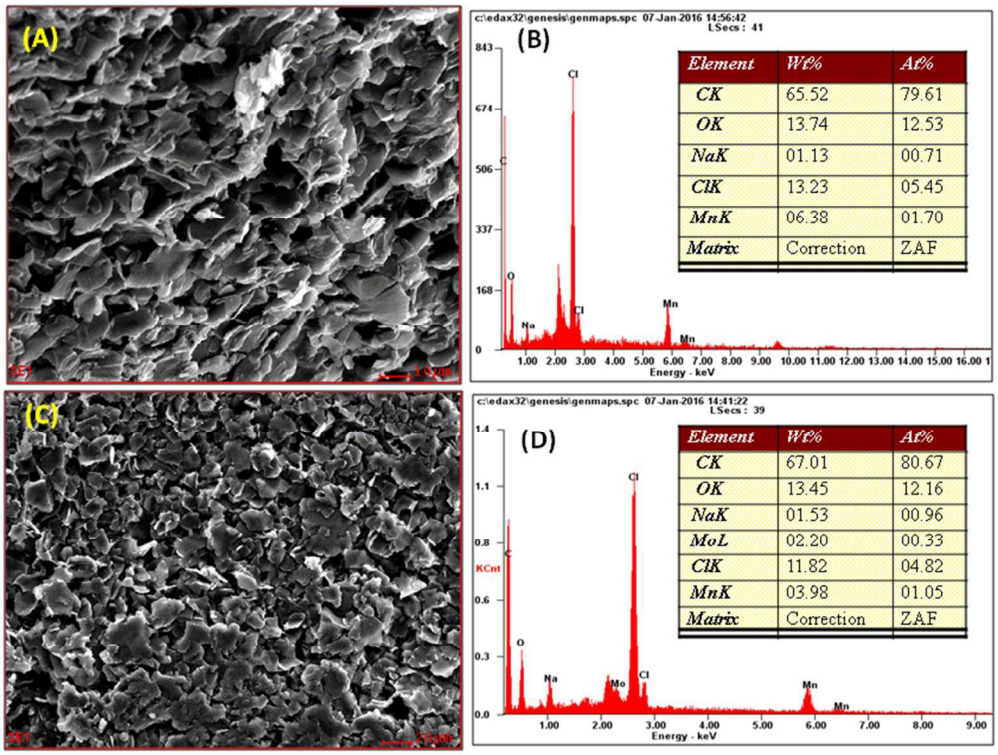

223x168mm (96 x 96 DPI)

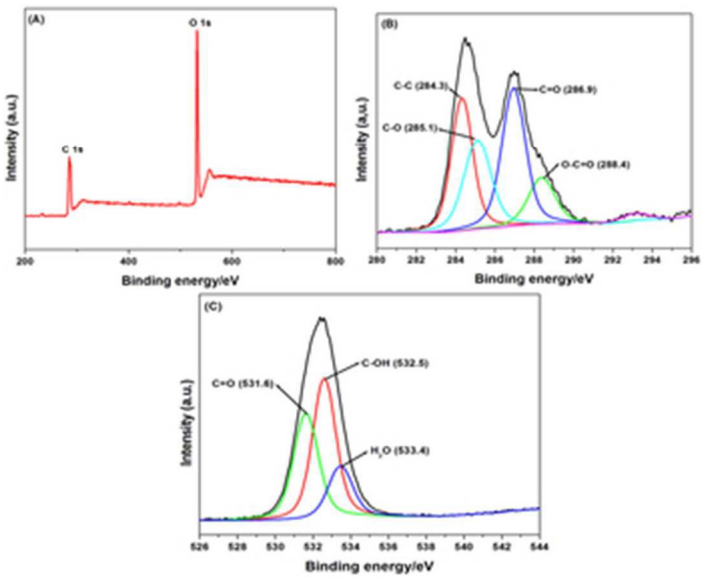

29x24mm (300 x 300 DPI)

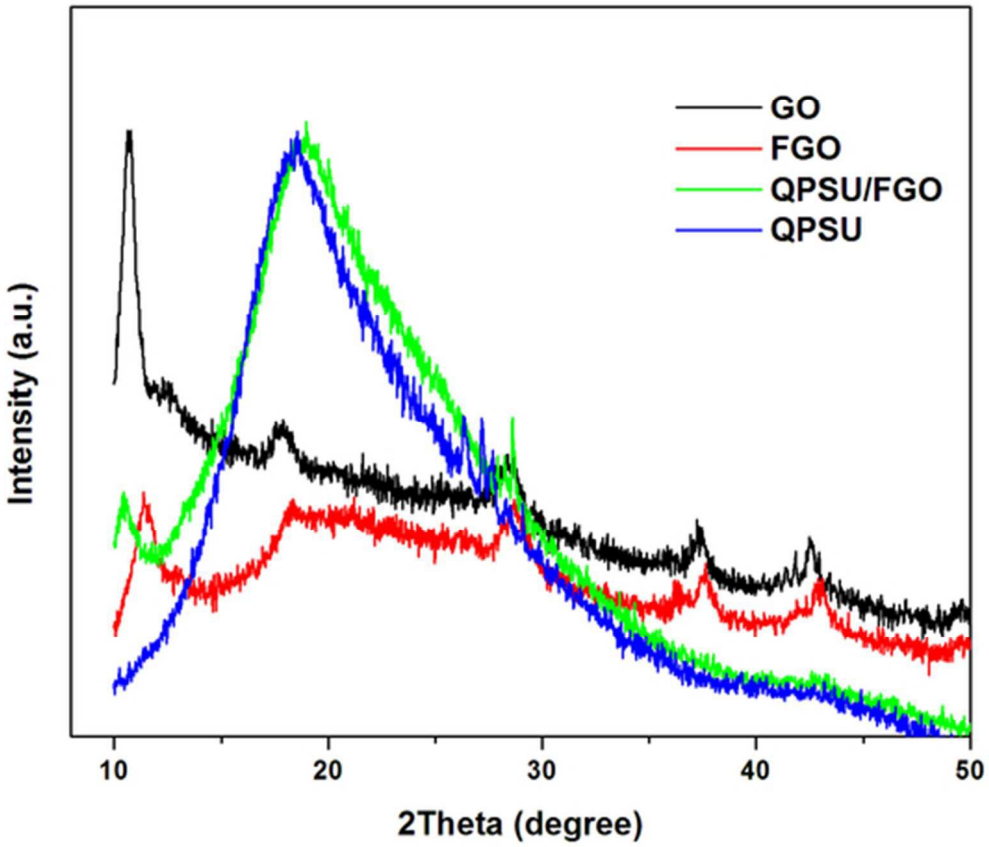

45x39mm (300 x 300 DPI)

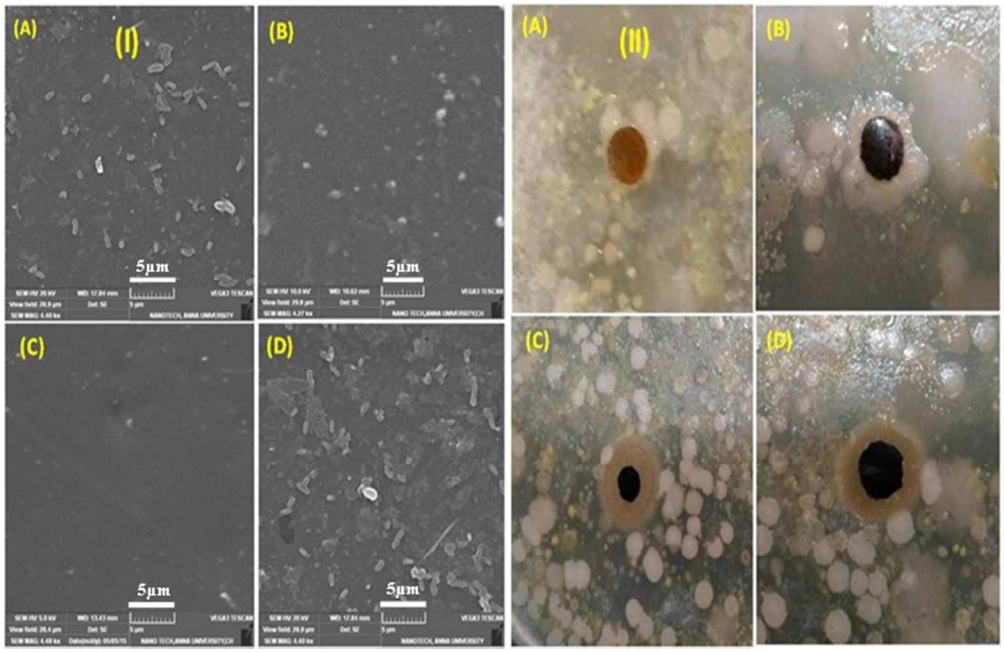

204x131mm (96 x 96 DPI)

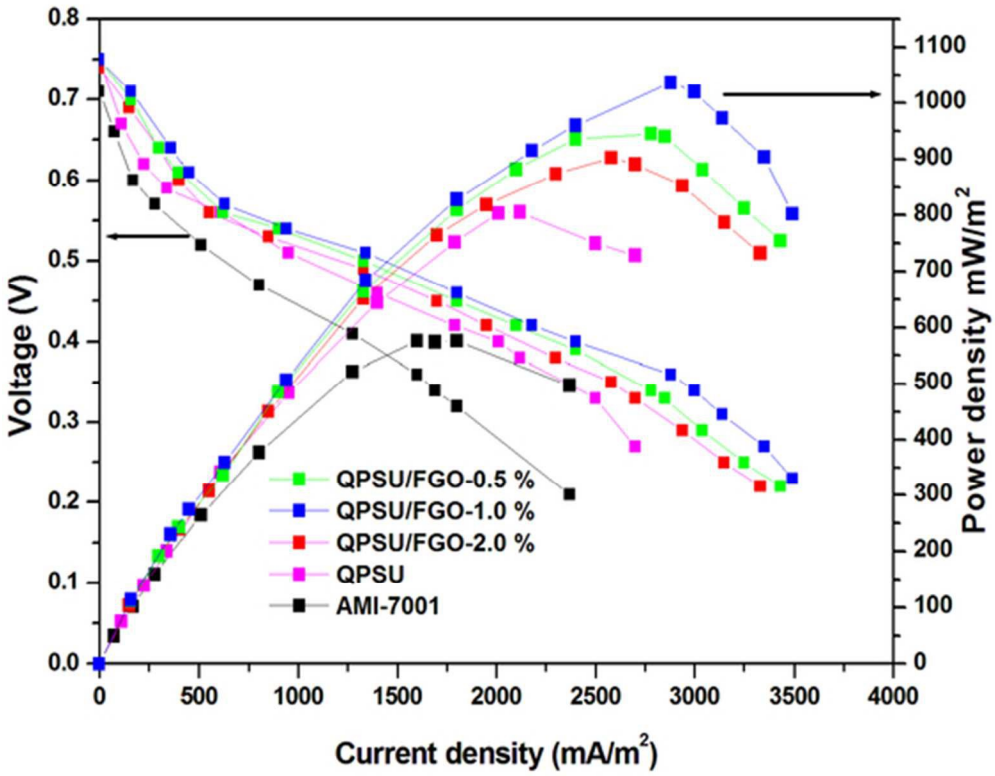

48x38mm (300 x 300 DPI)

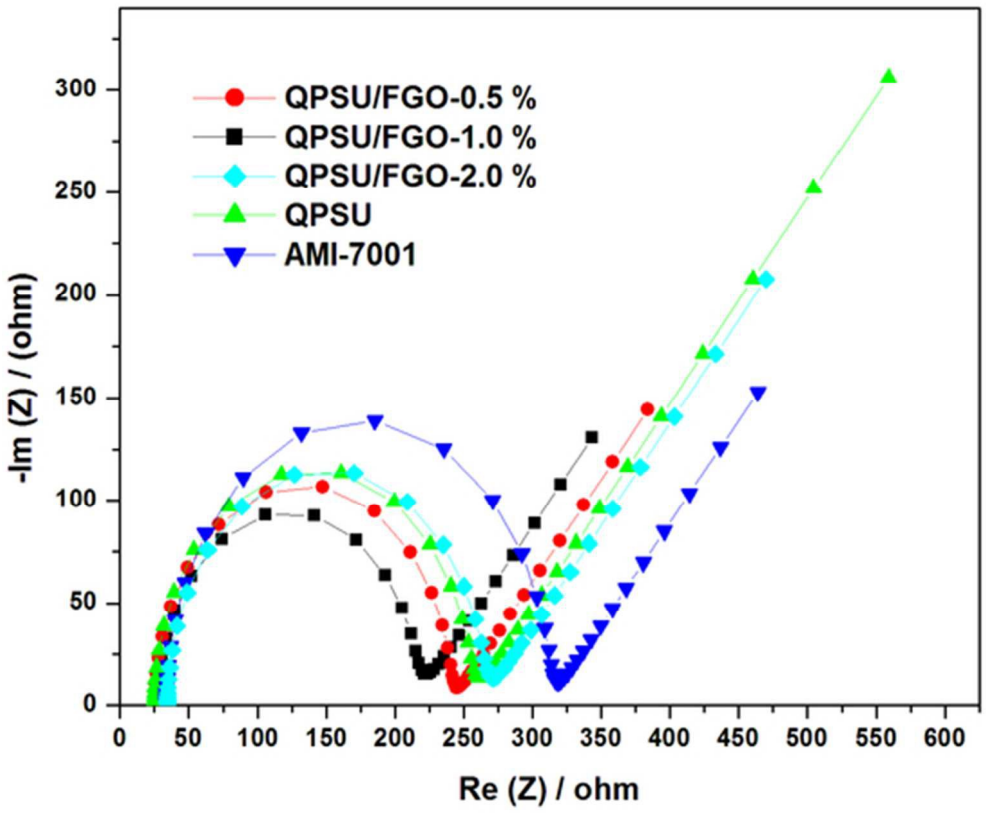

46x39mm (300 x 300 DPI)

A Facile Modification of Poly sulphone based Anti biofouling Anion Exchange Membrane for Microbial Fuel Cell Application

*Elangovan Mahendiravarman and Dharmalingam Sangeetha**
Department of Mechanical Engineering, Anna University, Chennai-600 025, India
*Corresponding author Email: sangeetha@annauniv.edu
Tel No: +91-44-22357763, Fax No: +91-44-22357744

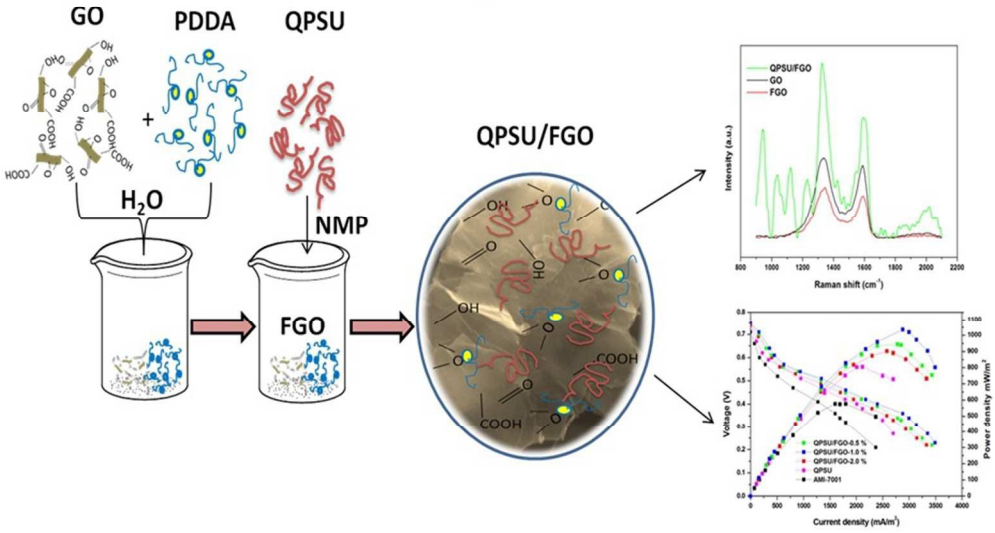

247x181mm (96 x 96 DPI)